

## Structural Transitions in Clathrate & Clathrate-like Compounds

Stefano Leoni, Wilder Carrillo-Cabrera and Yuri Grin

The structural motif of clathrates, where a periodic packing of condensed cages of atoms results in a framework hosting guest moieties, is found in many systems, like gas hydrates, alkali and alkaline earth metal silicides, germanides or stannides, and in several ternary and multi-component varieties as well. Guest-free examples are the silicas clathrasil and melanophlogite as well as some metal-free hypothetical modifications, interesting for their energetical closeness to diamond. The dual relationship of clathrates to sphere packing compounds dividing space into tetrahedra, like the Frank-Kasper structures, and the efficiency in filling space, while realizing a surface of minimal area, are additional properties of these structures. In connection with foams, clathrate I type provides a periodic arrangement of two polyhedral cells with minimal surface area.

The present report gives a summary of the investigations on structural transitions involving clathrate or clathrate-like covalent networks. The investigations serve three purposes:

- to learn, in a chemical context, how to take apart a clathrate structure,
- to further develop tools for modeling structural phase transitions,
- to provide order parameters for molecular dynamics calculations.

Periodic networks can be effectively described by Periodic Nodal Surfaces (PNS) [1]. A surface can either support the network, whereby the latter is a tiling of the former, or it can envelop the network in its labyrinths. In the context of structural phase transitions the limiting frameworks can be enveloped by periodic surfaces, and the transition can be realized as a distortion of one surface into the other [2, 3]. As the topology of the surface matches those of the networks, changes in surface topology hint at major changes in the networks, like bond-breaking or bond-formation [3].

A recently investigated compound,  $\text{Eu}_8\text{Ga}_{16}\text{Ge}_{30}$ , has been shown to exist in two modifications, a high temperature  $\beta$ -phase with the structure of clathrate I, and a low-temperature  $\alpha$ -phase of symmetry  $I\bar{4}3m$ , clathrate VIII [4]. The network of clathrate I is a packing of tetrakaidecahedra with dodecahedral interstices, whereby the former are stacked along, opening a system of channels in the network. The network of clathrate VIII is built up by 20-hedral cages, formed by three five-membered rings, three six-membered rings and three seven-membered rings. Their packing leaves back eight-hedral voids, empty in the structure. The topology of the labyrinths is beautifully described by periodic surfaces (Fig. 1). In both structures two europium atoms are positioned at the 3-fold axis,

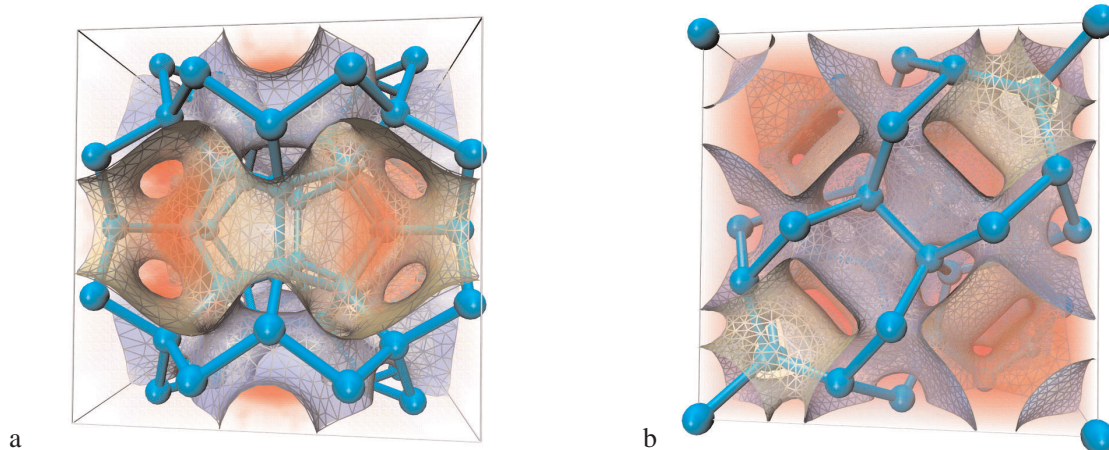


Fig. 1: Network of a) clathrate I and b) clathrate VIII in a labyrinth of a periodic surface.

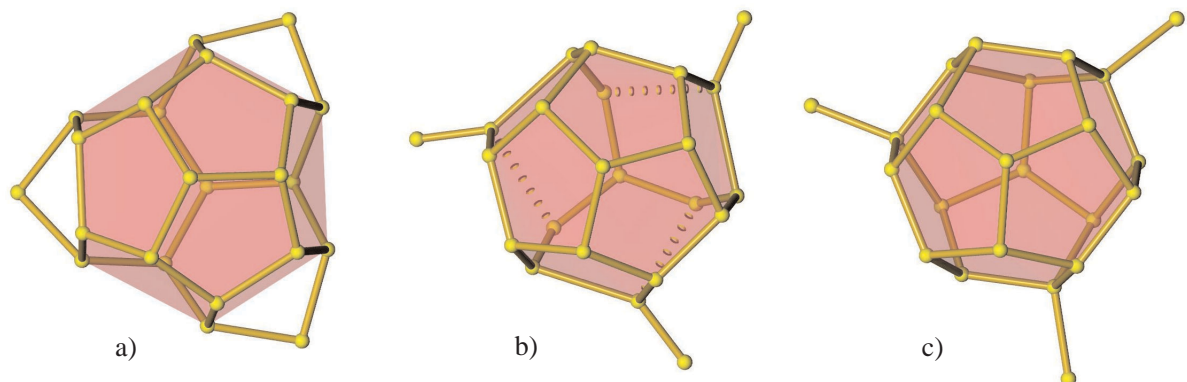


Fig. 2: a) 20-hedron in clathrate VIII, b) intermediate and c) icosahedron in clathrate I.

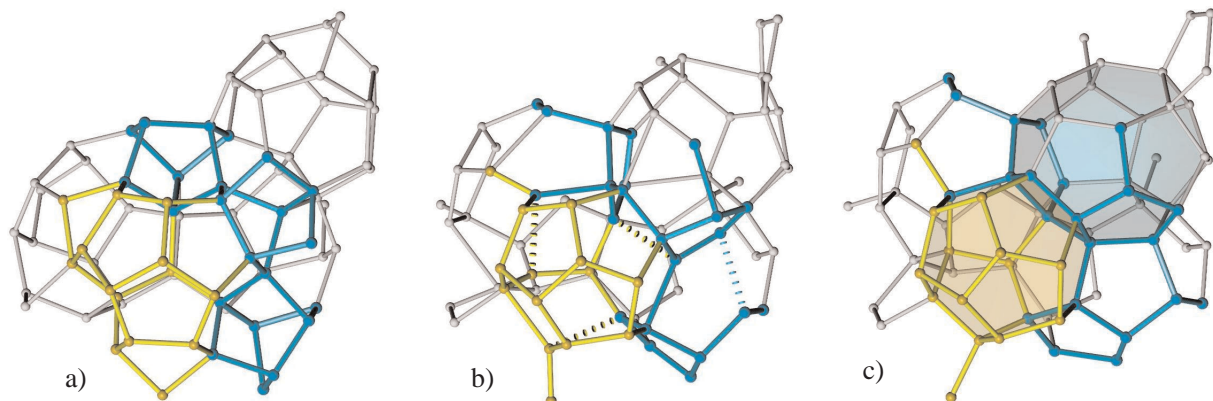


Fig. 3: a) 20-hedron and three 8-atoms cages in clathrate VIII, b) intermediate and c) icosahedron and tetrakaidecahedron in clathrate I.

so that a shift brings their positions into coincidence. As a network is required to remain within the same labyrinth while migrating from one surface to the other, a path linking the two structures can be formulated using the deformation of the labyrinths. Tracking the changes around the two crystallographically different Eu positions in clathrate I provides a picture of the transition in terms of distortions of polyhedra (Figs. 2 and 3). The dodecahedra are locked on 3-fold axes. Their interconversion involves the synchronous but opposite rotation of the upper and lower halves of the polyhedron, as illustrated in Fig. 2. The atoms forming the tetrakaidecahedra rearrange into a 20-hedron and an 8-hedron, as it is illustrated in Fig. 3. Interestingly, the process begins by opening the six-membered rings and with that, by destroying the channel system. The corner-connected 8-hedra of the clathrate VIII structure end up in a stripe of adjacent, edge-sharing five-membered rings, whereby only one five-membered ring of the original 8-atoms cage is conserved.

The atomistic model can be further refined by fully exploiting the topological information provided by the surfaces. In a common supergroup,  $Im\bar{3}m$ , a surface close to Schoen's minimal surface  $I$ -WP can be calculated, whose two labyrinths separate an  $I$  from a  $NbO$  net, as shown in Fig. 4b. In clathrate VIII, a  $NbO$  net is built by the (empty) centers of the 8-hedra. The two nets can be shown to represent the most simple prototypes for both structures, clathrate I and clathrate VIII, and to underlie the entire transition. In the sense of a hierarchical replacement [5], nodes of a basic net are substituted by more complicated aggregates of atoms. In clathrates VIII, each node of the  $NbO$  net is replaced by an 8-atoms cage. On the other side of the surface (Fig. 4a) a centered tetrahedron with double-capped edges (17 atoms in total) is located on the  $I$  net. The capping vertices are shared with the cages on the  $NbO$  net (Fig. 4a). The aggregate of 17 atoms results from six five-membered rings meeting at a common vertex. A shorthand notation is provided by graph theory, where such a graph is

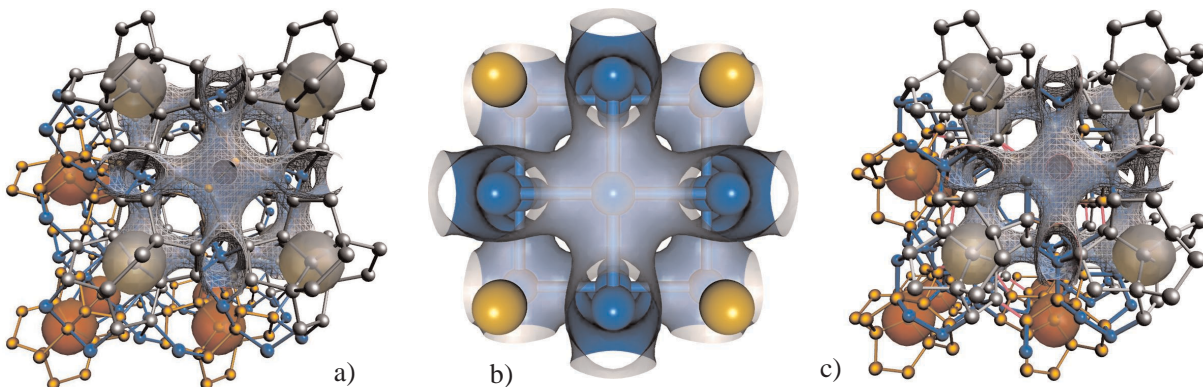


Fig. 4: a)  $K_5$  fragments placed on the centers of an  $I$  configuration in clathrate VIII; b) Schoen I-WP minimal surface; c)  $K_5$  fragments taking on two different orientations in clathrate I.

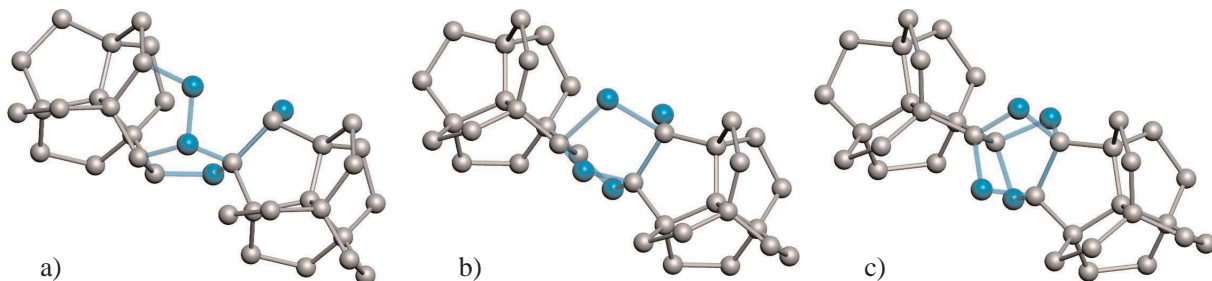


Fig. 5: Concerted rotation of two  $K_5$  fragments. a) clathrate I, b) intermediate, c) clathrate VIII.

referred to as  $K_5$ . In clathrate I, the  $I$  net splits into a  $P$  and a  $P_{\frac{1}{2}\frac{1}{2}\frac{1}{2}}$  net. The same replacement as for clathrate VIII can be made, but the  $K_5$  fragments take on two possible orientations with respect to one distinct 3-fold axis,  $+\alpha$  and  $-\alpha$  (Fig. 4c). If the  $K_5$  fragments are considered as rigid, the only tunable parameter of the transition is the angle  $\alpha$ . The concerted rotation of the  $K_5$  fragments triggers the opening of the cages on the other side of the surface, which in clathrate I are strongly distorted (Figure 5a-c). The common space group of all intermediates can be shown to be  $R3c$ .

The new compound  $\alpha\text{-BaAl}_2\text{Ge}_2$ ,  $\alpha\text{-BaCu}_2\text{S}_2$  structure type, shows a temperature dependent dimorphism: the 3D network of the low temperature  $\alpha$ -phase transforms into the layer structure of the high-temperature  $\beta$ -phase,  $\text{BaZn}_2\text{P}_2$  structure type. In the  $\beta$ -phase, the Ba atoms are encapsulated between puckered layers of  $\text{Al}_2\text{Ge}_2$ . Within the layers, the atoms are four-fold coordinated, Al tetrahedrally, while Ge is at the apex of a quadrangular pyramid, and both are facing Ge atoms of the next layer. The  $\alpha$ -phase shows a distorted network of

four-bonded Al and Ge atoms with large cavities, where Ba atoms are encapsulated (Fig. 6).

A mapping of the coordinates of the atomic positions of the two phases into each other and a path connecting them can be worked out. Similar to the

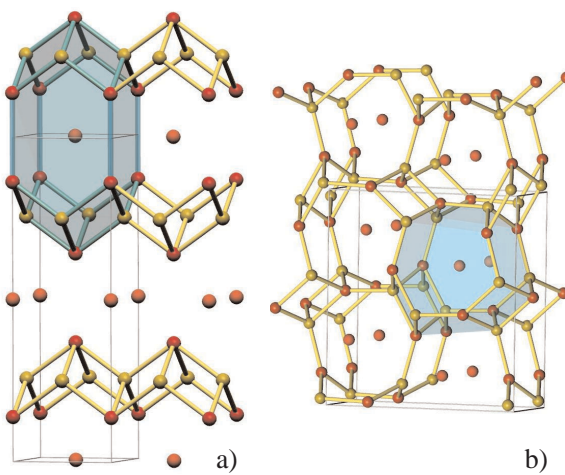


Fig. 6: Crystal structure of a)  $\beta\text{-BaAl}_2\text{Ge}_2$ , b)  $\alpha\text{-BaAl}_2\text{Ge}_2$ .

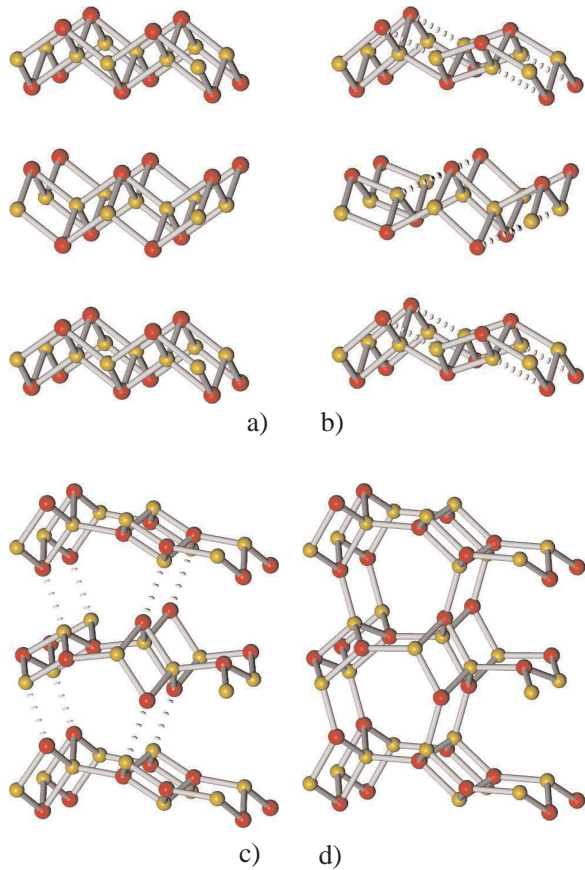


Fig. 7: Structural path connecting  $\beta$ - (a) to  $\alpha$ - $\text{BaAl}_2\text{Ge}_2$  (d). (b), (c) intermediates.

clathrate I-to-clathrate VIII transition, periodic surfaces can be used to envelop the networks of the  $\alpha$ - and  $\beta$ -modifications and reproduce their topology. Starting from the stacking of puckered layers of the  $\beta$ -phase, a set of parallel bonds is opened within each layer. The remaining interconnected zig-zag stripes (twisted double crankshafts) containing six-membered rings remind of the mineral Feldspar and of the Si net in Coesite, where the linkages along [001] are different, though. The rotation of each second strip between a layer causes the inter-layer Ge-Al contacts to become shorter, eventually resulting in bonds bridging the layers into the 3D network of the low-temperature phase (Fig. 7).

The topological information provided by periodic nodal surfaces and by calculation of the Electron Localization Function (ELF) [6] can be used to reinforce each other, with dramatic effects on the understanding of both the bonding situation and the structural relationship between the two modifications. In a most concise sense, the ELF fills in the details of the bonding that can only be foreshadowed by the nodal surface. For  $\beta$ - $\text{BaAl}_2\text{Ge}_2$ , a PNS shows the separation of the  $\text{Al}_2\text{Ge}_2$  from the Ba atoms, and suggests the layered nature of the compound. The valence basin set [7] of the germanium atom consists of five basins, four are located between Ge and Al atoms and one points towards

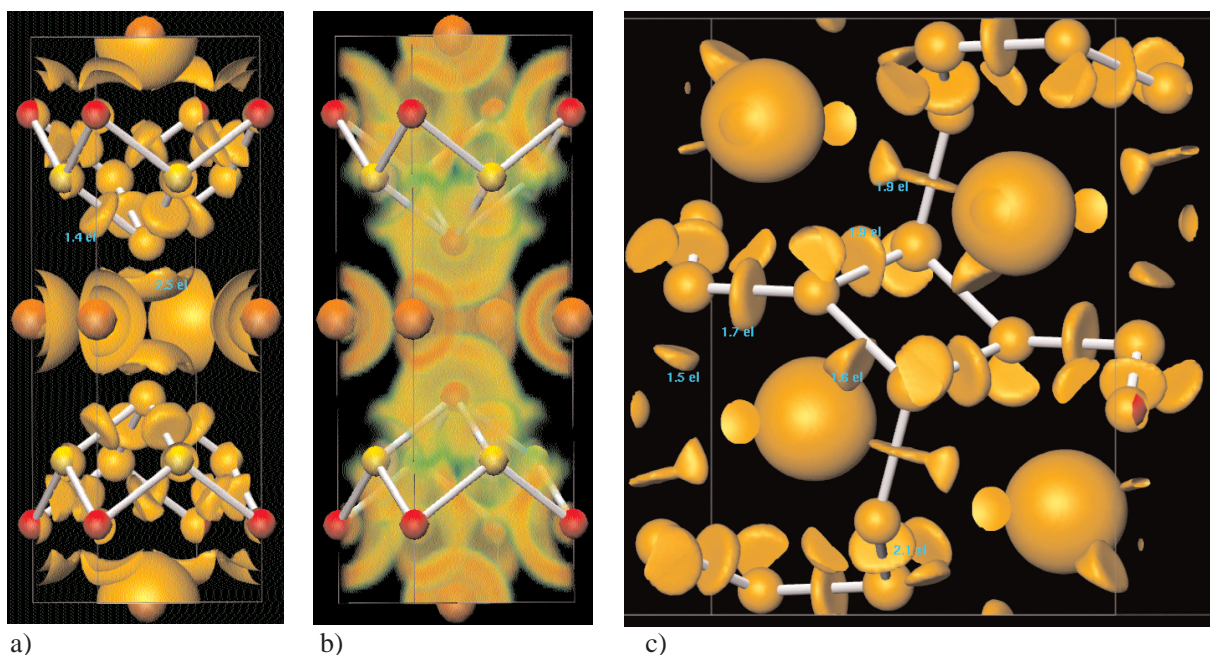


Fig. 8: ELF of  $\beta$ - $\text{BaAl}_2\text{Ge}_2$  (a,b) and  $\alpha$ - $\text{BaAl}_2\text{Ge}_2$  (c). Isosurface representation (a, c), volume representation (b).

the Ge atom the next layer (Fig. 8a). At a lower value of the ELF ( $\eta = 0.48$ ), the valence basin set of the  $\text{Ge}_2\text{Al}_2$  network is formed. The barium atoms remain separated from the network until  $\eta = 0.08$ . This clearly confirms the picture given by PNS. The isolation of the Ba atoms complies with the Zintl-Klemm electron counting scheme, where valence electrons should be transferred from Ba to the Al-Ge network. The distinction between the two phases, truly topological, is out of the scope of the counting scheme. The interplay of periodic surfaces and ELF is invaluable in tracing a sharp line between the two phases.

Calculation of periodic surfaces and ELF produces (large) volume data of scalars. Traditionally, such datasets have been visualized through the interpolation of surfaces at isovalue. Isosurfaces represent a small amount of the dataset, though, and fail to reveal important details. Using volume rendering algorithms, the whole dataset can be visualized and important details represented within the same picture (Fig. 8b). Novel techniques, like multiresolution textures and ray casting, scalar and gradient opacity functions are providing exciting perspectives and new insight from scientific visualization.

The scaffolding of periodic surfaces, applied to structural phase transitions, is able to provide a most valuable path and mechanistic model connecting topologically different networks and atomic arrangements. This is being used as input coordinates for molecular dynamics simulations. Using intermediates as starting point allows the calculation of physically meaningful atomistic paths within typical MD simulation times.

## References

- [1] H.G. von Schnerring, R. Nesper, *Z. Phys. B* **83**, 407 (1991).
- [2] R. Nesper, S. Leoni, *ChemPhysChem* **2**, 413 (2001).
- [3] S. Leoni, R. Nesper, *Acta Crystallogr. A* **56**, 383 (2000).
- [4] S. Paschen, W. Carrillo-Cabrera, A. Bentien, V.H. Tran, M. Baenitz, Y. Grin, F. Steglich, *Phys. Rev. B* **64**, 214404 (2001).
- [5] J.-F. Sadoc, R. Mosseri, *Geometrical Frustration*, Cambridge, University Press, Cambridge 1999.
- [6] W. Carrillo-Cabrera, N. Caroca-Canales, H.G. von Schnerring, *Z. Anorg. Allg. Chem.* **620**, 247 (1994).
- [7] A.D. Becke, K.E. Edgecombe, *J. Chem. Phys.* **92**, 5397 (1990).
- [8] A. Savin, O. Jepsen, J. Flad, O.K. Andersen, H. Preuss, H.G. von Schnerring, *Angew. Chem. Int. Ed.* **31**, 187 (1992).
- [9] M. Kohout, F.R. Wagner, Yu. Grin, *Theor. Chem. Acc.* **108**, 150 (2002).